Heliyon 7 (2021) e06194

Contents lists available at ScienceDirect

Heliyon

journal homepage: www.cell.com/heliyon

Research article

Disentangling multiple PM emission sources in the Po Valley (Italy) using honey bees

Giancarlo Capitani [a], Giulia Papa [b], Marco Pellecchia [c], Ilaria Negri [b,*]

[a] DISAT – Università Milano Bicocca, Milano, Italy
[b] DIPROVES – Università Cattolica del Sacro Cuore, Piacenza, Italy
[c] KOINE'– Consulenze Ambientali, Montechiarugolo, Parma, Italy

ARTICLE INFO

Keywords:
Honey bee
PM sensors
SEM/EDX
Agriculture
Waste incineration
Vehicular traffics

ABSTRACT

Particulate matter (PM) is a complex mixture of airborne chemical compounds commonly classified by their aerodynamic diameter. Although PM toxicity strongly depends on the morphology, chemical composition, and dimensions of particles, exposure limits set by environmental organisations only refer to the mean mass concentration of PM sampled daily or annually by monitoring stations.

In this study, we used honey bees as sensors of airborne PM_{10} and $PM_{2.5}$ in a highly polluted area of the Po Valley, northern Italy. Honey bees are an efficient sampler of airborne PM because, during flight and foraging activities, their pubescence promotes the accumulation of electrical charge on the body surface owing to air resistance, thus enhancing airborne PM attraction. Particles attached to the body of bees are readily accessible for physico-chemical characterisation using a scanning electron microscope coupled with X-ray spectroscopy (SEM/EDX). Our results demonstrate that residents in the study area are intermittently but chronically exposed to a well-defined spectrum of metal-bearing particles and mineral phases known to induce specific health outcomes.

The morphology, size, and chemical composition of PM_{10} and $PM_{2.5}$ detected on bees in the monitoring area were indicative of traffic, agricultural operations, and high-temperature combustion processes. The contribution of the A1 Milano-Bologna highway, local wheat and alfalfa cultivation, and the Parma incineration plant were clearly distinguishable. Our data also demonstrated that PM exposure levels may vary sharply throughout the year based on recurrent local activities.

1. Introduction

Particulate matter (PM) is an air pollutant consisting of a mixture of suspended solid and liquid particles that originate directly from natural sources (e.g., volcanic eruptions, forest fires, and sea spray) and anthropogenic sources (e.g., motor vehicles, factories, and agriculture) and indirectly from chemical reactions that convert atmospheric precursors into secondary PM. Airborne PM is commonly classified according to particle size; inhalable PM includes particulates with an aerodynamic diameter $\leq$10 μm (PM_{10}), which can penetrate the respiratory tract below the larynx, while respirable PM $\leq$ 2.5 μm ($PM_{2.5}$) may penetrate the gas-exchange region of the lungs (Brown et al., 2013).

The human health hazards associated with PM exposure are universally acknowledged both in terms of the effects of their components and the enhanced transmissibility of pathogens (Wang et al., 2014; Setti et al., 2020; van Doremalen et al., 2020). Although the toxicity of PM strongly depends on its morphology, chemical composition, and dimensions (Wang et al., 2014; Maher et al., 2016; Bencsik et al., 2018), exposure limits set by environmental organisations only refer to the mean mass concentrations of PM sampled daily or annually at monitoring stations, with no specific indicators regarding the chemical nature of the particles (see, for example, Directive 2008/50/EC of the European Parliament and of the Council of 21 May 2008 on ambient air quality and cleaner air for Europe).

In the present study, honey bees (*Apis mellifera* L.) were used as an alternative sampling system for airborne PM_{10} and $PM_{2.5}$ in a highly polluted area of the Po Valley, northern Italy, near the city of Parma. Besides being a key provider of ecosystem services through the provision of many products, such as honey, pollen, wax, and propolis, and the pollination of many wild and cultivated plants, honey bees are important bioindicators of environmental contamination (Devillers and Pham-Delegue, 2002; Bargańska et al., 2016). Bees and their products are

* Corresponding author.
E-mail address: ilaria.negri@unicatt.it (I. Negri).

https://doi.org/10.1016/j.heliyon.2021.e06194
Received 16 June 2020; Received in revised form 28 June 2020; Accepted 1 February 2021

commonly used for the detection of environmental pollutants including pesticides, heavy metals, radionuclides, volatile organic compounds, polynuclear aromatic hydrocarbons, and dioxins (Devillers and Pham-Delegue, 2002; Giglio et al., 2017; Perugini et al., 2011; Goretti et al., 2020).

Recent studies have demonstrated that forager bees act as efficient mobile samplers for airborne PM (Negri et al., 2015; Pellecchia and Negri, 2018; Papa et al., 2020). During flight and foraging activity, bee pubescence promotes the accumulation of electrical charge at the body surface owing to air resistance. This charging enhances the attraction of airborne particles, which include not only pollen but also pollutants (Vaknin et al., 2000; Bonmatin et al., 2015). Airborne PM attached to bee bodies can be analysed based on size, morphology, and chemical composition using a scanning electron microscope (SEM) coupled with X-ray spectroscopy (EDX) (Negri et al., 2015; Pellecchia and Negri, 2018). SEM/EDX is a powerful, fast, and non-destructive analysis technique, and determining both the chemical and morphological characteristics of particles typically allows their accurate identification and classification. Single particles can also be counted and their size measured for detailed quantitative assessment. In the present study, we applied this methodology to investigate PM_{10} and $PM_{2.5}$ accumulated on honey bees in an urban area of the Po Valley, which is one of the most important industrial and agricultural areas in Italy and Europe, characterised by a high population density and low air quality (Marcazzan et al., 2001; Pirovano et al., 2015).

The study area includes agricultural fields, a relatively new incinerator plant, and a stretch of the Milano-Bologna motorway. A single fixed monitoring station for the airborne concentrations of gaseous pollutants and PM has been established, providing daily and annual mean concentrations of PM_{10} and $PM_{2.5}$ particles per cubic metre of air volume, but no information on the nature and chemical composition of the particles is currently available (Regional Environmental Protection Agency, www.arpae.it).

We aimed to test the use of SEM/EDX for characterising the morphology, chemical composition, and size of PM collected by bees and distinguishing among different emission sources to, ultimately, estimate their relative contributions in the study area. The EDX spectra associated with multiphase aggregations and sub-micrometre PM are also explored.

2. Materials and methods

2.1. Study area

A hive was placed in the N-NE peri-urban area of the City of Parma approximately 4 km from the city centre (Figure 1a). The hive was placed on a grassy lot surrounded by cultivated fields approximately 100 m from the A1 motorway, 400 m from the Parma exit, and 400 m from the incinerator plant (Figure 1b). The A1 motorway connects Milan and Naples and is one of the most congested motorways in Italy, experiencing an average traffic load of over 2.5 million vehicles per month.

The local nectar and pollen resources for the bees included several wild plant species (e.g., *Taraxacum officinale*, *Prunus spinosa*, and *Brassicaceae*) and crops including corn, alfalfa, and rapeseed, and the apiary was surrounded by wheat and alfalfa fields (brown plots in Figure 1b).

In addition to a system that continuously monitors stack emissions from the incinerator (e.g., carbon monoxide and dioxide, nitrogen oxides, hydrogen fluoride, hydrogen chloride, ammonia, and dust), PM_{10}, $PM_{2.5}$, mercury, benzene, toluene, xylene, and ozone are regularly monitored in the area through fixed and mobile monitoring stations (Regional Environmental Protection Agency, www.arpae.it). In this study, airborne PM was monitored from June to October, 2017 using honey bees.

2.2. Geological setting

Parma is located in the central Po Valley in a Pliocene/Quaternary alluvial sedimentary plain between the northern Apennines and the Southern Alps (Figure 2). The study area includes terraced alluvial fan deposits built up by the hydrographic network of the Taro River and the Parma Stream, both tributaries of the Po River that flows north of Parma. These terrains are distinguished on a morphological, archaeological and pedostratigraphic basis into the Ravenna subsynthem and the Modena Unit (Calabrese and Ceriani, 2009). The Ravenna subsynthem primarily comprises gravels and sandy gravels with local intercalations of sands and silty sands covered by a silty-clay layer of variable thickness. The roof alteration front is moderately thick (0.1–1 m) and the soils show a shallow decarbonated layer. The Modena Unit primarily comprises sands with pebbly lenses and levels covered by a discontinuous silty layer. The roof alteration front is moderately thick (a few tens of centimetres) with an overall thickness of 5–6 m and (Calabrese and Ceriani, 2009).

2.3. Sample collection and preparation

The beehive was installed in the study area in February 2017 and worker bees were collected from June to October during warm weather when they are more active and forage across an average area with a radius of about 3 km. Approximately five worker bees were collected on a monthly basis in June, July, August, and October, yielding a total of 20 bees. In September, bees were not sampled owing to the treatments applied by the beekeeper against the ectoparasitic mite *Varroa destructor*.

Negative control bees consisted of newly eclosed individuals from a brood frame kept in a growth chamber. Briefly, a brood frame was selected and placed in an incubator at 36 °C and 60% relative humidity for approximately 16 h. Newly eclosed adults were randomly selected and prepared for SEM/EDX analyses. Once collected, worker bees were immediately placed in soda-glass capped vials, stored on ice to keep them inactive, and rapidly brought to the lab for sample preparation. Preliminary studies have shown that PM on the bees is mostly concentrated along the costal margin of the forewings, medial plane of the head, and inner surface of the hind legs (Negri et al., 2015). In this study, we examined the forewings, which are relatively easy to explore with the SEM probe owing to their flatness and lack of long setae (Pellecchia and

Figure 1. Location of the hive relative to the city centre of Parma (a) and the incinerator plant and the motorway (b).

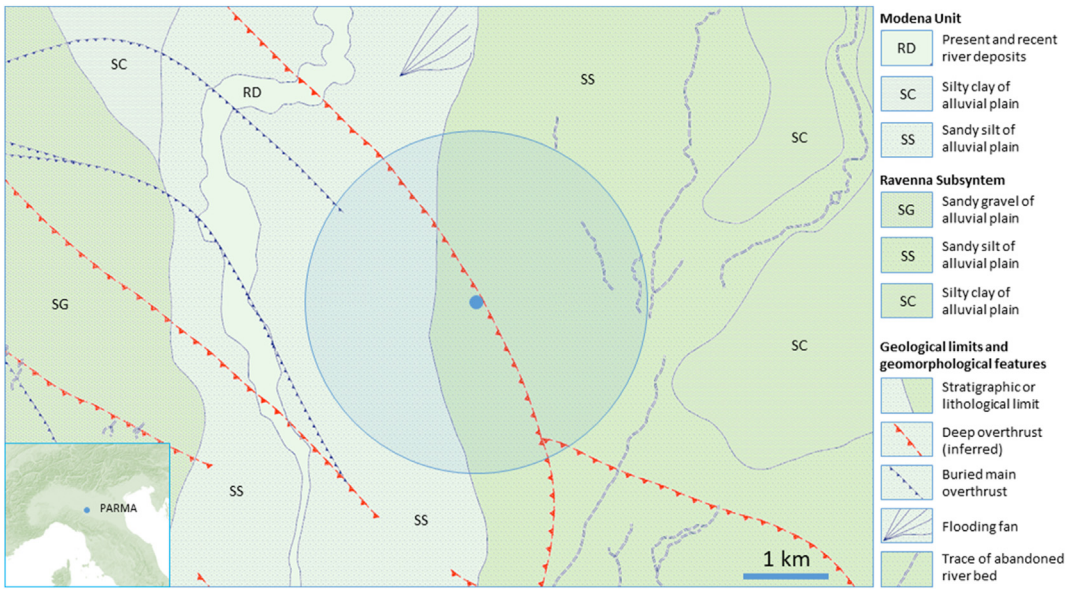

Figure 2. Geological map of the area around the hive (small circle). The shaded area represents the average area explored by the worker bees during their foraging activities during warm weather. Based on a map of the Emilia-Romagna Region available at: http://geoportale.regione.emilia-romagna.it/it/mappe/informazioni-geoscientifiche/geologia/carta-geologica-1-50.000.

Negri, 2018). The bees' wings were cut under a stereoscope with a scalpel and mounted onto SEM stubs using double adhesive carbon tape. Before the SEM/EDX investigation, because of the insulating properties of the samples, the stubs were carbon coated to make them conductive to avoid charging flare during the observations. Moreover, haemolymph (blood) was extracted from the control bees by puncturing the dorsal aorta, following the method standardised by Garrido et al. (2013), to distinguish the potential contribution of the haemolymph (that permeates the wings) to the EDX spectra; haemolymph droplets were set and dehydrated upon stubs under a sterile hood, graphitised, and analysed using SEM/EDX.

2.4. SEM/EDX analyses

The SEM/EDX investigation was performed using a Zeiss Gemini 500 field-emission instrument equipped with a Bruker XFlash 6130 EDX micro-analyser. A panoramic electron backscattered (BSE) image was acquired for each analysed area along with magnified images of some particles representative of the different phases encountered. Each analysed particle was attributed to a phase (or phase aggregate) based on the elements present in the corresponding spectrum as well as the relative amounts and morphologies of the particles themselves. For instance, different minerals were characterised and distinguished based on elemental compositions; clay minerals generally have a pronounced lamellar habit in addition to a given elemental content; halides have a cubic habit as well as some sulphides that, in turn, feature distinct elemental signals. While this methodology is rapid, cost-effective, and able to reveal nano-sized particles, it has the following limitations: (1) the EDX system is not very sensitive to light elements such as hydrogen and carbon. Therefore, hydrocarbon molecules cannot be efficiently identified and characterised; (2) BSE imaging is sensitive to the average atomic number of the particles. Therefore, heavy particles can most easily be recognised on light organic substrates, including bee wings, while conversely, light particles show poor contrast and tend to be underestimated; (3) even when nanometre-scale image resolutions are obtained under optimal experimental conditions, the spatial resolution of the EDX probe is only few microns. Therefore, for particles smaller than the EDX probe—namely PM with an aerodynamic diameter less than 2–3 μm—the surroundings will always contribute to the resultant spectrum. As such, we could obtain the average composition of the mixture small-particle aggregates; and (4) different mineral species may have the same elements in different proportions, and the only way to distinguish them is to determine the atomic proportions. For example, forsterite (Mg_2SiO_4) can be distinguished from enstatite ($MgSiO_3$) based on their respective Mg/Si ratios of 2:1 and 1:1. Such determinations are straightforward for ideal samples (i.e., with a flat and polished surface and of sufficient size to entirely contain the electron beam interaction volume i.e., <10 μm^3); however, for non-ideal samples, raw data cannot be properly reduced, that is, intensity data cannot be properly transformed into concentrations. In our case, most particles had an irregular shape, rough surfaces, and were smaller than the EDX probe, meaning that interpretation was sometimes more difficult. The airborne particles on the honey bee wings were also analysed in terms of the number of particles per surface area and their size distribution using the image-processing software 'Digital-Micrograph' (Gatan Inc., Pleasanton, CA, USA). Briefly, 12 SEM-BSE images randomly chosen among the obtained pictures with a homogeneous background and magnifications ranging from 1.14 KX and 25.38 KX were considered. Particles that could be distinguished from the background (i.e., the honey bee wing) based on brightness and contrast were selected and counted, and their morphological parameters were measured. The PM mass was estimated assuming an average particle density of 2.65 g/cm^3 (corresponding to the density of quartz, which is the dominant mineral in soils; Rühlmann et al., 2006), and a measured mean circular particle diameter of 0.75 μm.

3. Results

3.1. Particulate matter analysis

In the negative controls, the electronic scan did not detect any PM contamination (Fig. S1); the experimental bees displayed contamination with inorganic dust typically <10 μm in diameter. The number of particles/mm^2 identified using the image-processing software varied from 2,724 to 511,121 (mean = 10,819), and images with a higher magnification displayed more particles (Fig. S2). The grain-size distribution of the identified particles is shown in Figure 3, which shows an exponential decrease in the number of particles with grain size. The estimated mass of PM per mm^2 was approximately 1.90 ng.

Most of the PM_{10} and $PM_{2.5}$ were identified as quartz, phyllosilicates, calcite, and feldspars. Figure 4 presents the crystal morphology and EDX

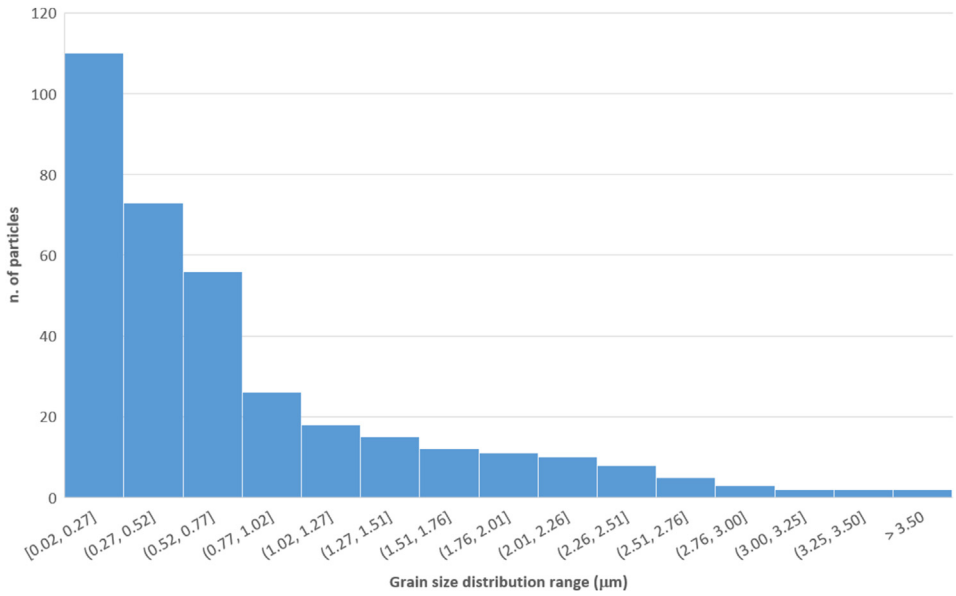

Figure 3. Grain-size distribution of PM detected on honey bee wings obtained via SEM-BSE image processing.

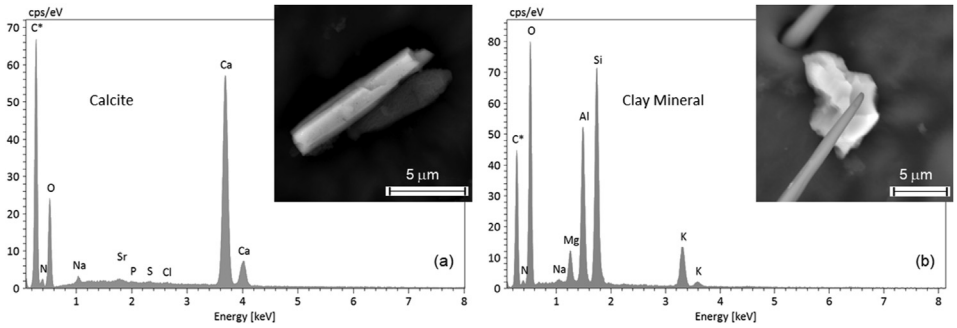

Figure 4. Sample 14/10: (a) EDX spectrum of an acicular calcite PM_{10} particle ($CaCO_3$; inset). Small amounts of Na and Sr may be present in calcite. Minor N, P, S, and Cl peaks are attributable to the bee wing; (b) EDX spectrum of a clay mineral particle (inset) consistent with illite $(K(Al,Mg,Fe)_2(Si,Al)_4O_{10}(OH)_2)$.

spectra of calcite and clay minerals, whereas some reference spectra for all these mineral phases are provided in Figs. S3 and S4. Spherical dust PM with a SiO_2 composition was also detected (Figure 5a), the morphology of which suggested anthropogenic origin. Other particles frequently found on bees included Fe-bearing compounds, such as Fe oxides, metallic Fe, and Fe alloys (Fig. S4). Barium sulphate was present in all samples, generally as a sub-micrometre fraction (Figure 5b). Other metallic particles including Cu, Al, and titanium oxide, were occasionally detected (Fig. S4). Phosphorous was ubiquitous in the studied samples, generally being detected in association with N, Cl, S, and several other elements (see below) and, in one case, having a spectrum consistent with apatite $[Ca_5(PO_4)_3(OH,F,Cl)]$.

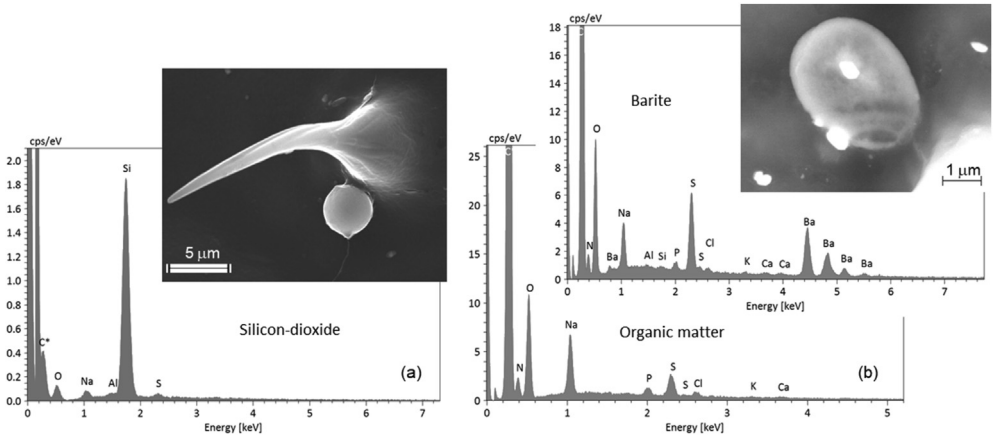

Figure 5. Sample 22/06: (a) Spherical SiO_2 particle of possible anthropogenic origin and its EDX spectrum; (b) Sub-microscopic particles of barite (white) distributed on a honey bee wing and a globular particle of possible organic matter with a complex accessory element association in which Na is dominant.

The EDX analysis of sub-micrometre particles was systematically affected by the signal from the bee wings, as outlined in the experimental section. Thus, to account for the contributions of wings to the overall EDX spectra, point analyses were performed directly on the wing membranes. The resulting spectra showed significant N, Si, P, S, Cl, K, ±Al, ±Na, ±Mg, and ±Fe peaks (Figure 6a). These peaks were systematically present for almost all of the analysed particles in proportions that roughly depended on particle dimension, i.e., the smaller were the particles, the higher were the wing-related peaks (Figure 6b–d). Most of the elements contributing to the spectra of small particles also reflected the EDX spectrum of the insect haemolymph samples (Figure 7).

3.2. Multiphase particles

In many cases, spectral interpretation was complicated by the multiphase nature of the particles, with constituent single phases being smaller than the total analysed volume. In such cases, phase identification can be ambiguous since different proportions or various phases may lead to the same average composition. Thus, compositional analysis can be employed to ensure more accurate spectral interpretation, as shown in Figure 8. Herein, the BSE images and elemental distributions show that the PM_{10} particles comprise at least three different major phases and contribute to the whole spectrum. The upper left particle primarily contains Si, Al, K, and Fe, likely being a clay mineral such as illite, with sub-microscopic inclusions of Fe oxides; the lower right particles primarily contain Na, S, Cl, and Ca, although Na and Ca are present in much greater abundance suggesting these elements may be combined with C to form secondary oxalates. In other cases, the different phases were easily distinguished by the BSE imaging, as in Figure 9 where clay minerals associated with organic matter are shown. The two different materials yielded different EDX spectra. For example, the P, S, and Na peaks were much higher in the organic matter spectrum than in the clay mineral one, suggesting that P, S, and Na were more highly concentrated in the former, and the small peaks in the clay mineral spectrum were spurious. Analogously, the small Si and Al peaks in the organic matter spectrum are considered to be spurious peaks originating from the clay minerals.

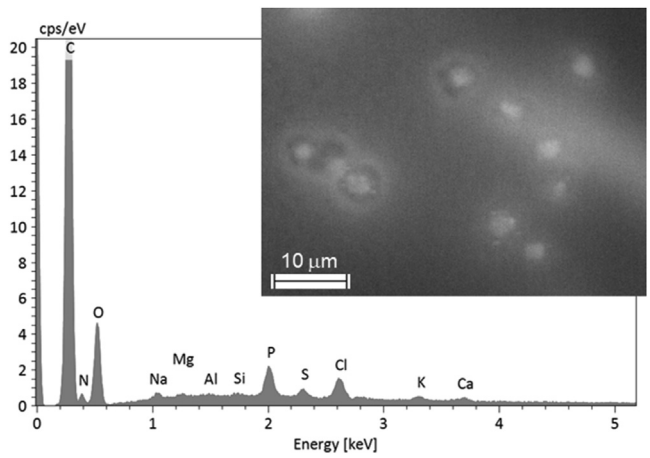

Figure 7. Representative EDX spectrum of the haemolymph of the control bees displaying significant levels of N, Na, P, S, Cl, K, and Ca, and trace amounts of Mg, Al, and Si (in addition to abundant C and O). Most of these elements were recurrent in the analyses of all fine particles, although in different proportions. Bright spots are likely insect hemocytes (i.e., insect "blood" cells). The spectrum refers to the ensemble.

3.3. Mineral phase distributions over time

Quartz was as abundant as calcite and clay minerals, and more abundant than feldspar (Figure 10). Clay minerals and calcite were more abundant on the bees collected in June and October, accounting for approximately 75% of the acquired spectra. In June, the ratio between clay minerals and calcite was 1.3:1; conversely, in October, calcite was more than twice as abundant as clay. In July and August, the percentage of clay minerals and calcite was lower than in June and October, decreasing to approximately 56% and 36%, respectively (Figure 10). Fe-bearing PM appeared rarely on bees collected in June (2%), more commonly on those collected in July (13%), and peaked on those collected in August (about 50%). In October, Fe compounds comprised approximately 12% of the total obtained spectra (Figure 10). A relatively

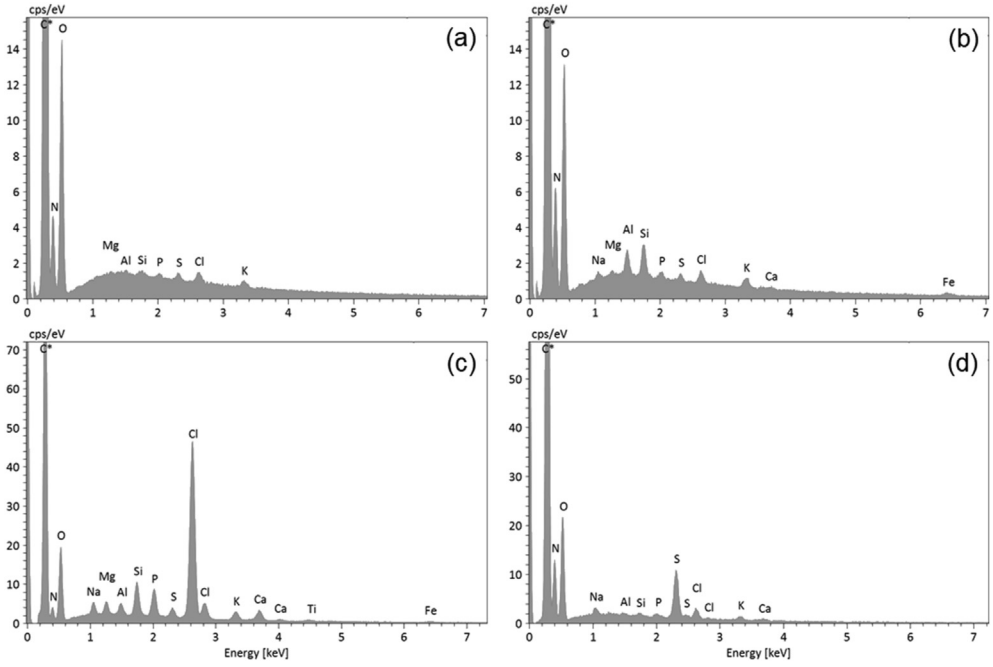

Figure 6. EDX spectra of sample 22/06: (a) Representative spectrum of the honey bee wing taken away from visible particles. Note the presence of small Mg, Al, Si, P, S, Cl, and K peaks in addition to the larger C, N, and O peaks; (b) Spectrum of a very small clay mineral particle. Note the increased Mg, Al, Si, and K peaks and the appearance of Na, Ca, and Fe peaks, all of which are elements typical of clay minerals; (c) Spectrum dominated by Cl (after C) possibly relating to a chloride condensed on a clay mineral particle (note the presence of related elements) along with P and S compounds; (d) Spectrum dominated by S and N peaks (after C and O peaks associated with the honey bee wing membrane) possibly indicating NOx- and SOx-derived compounds.

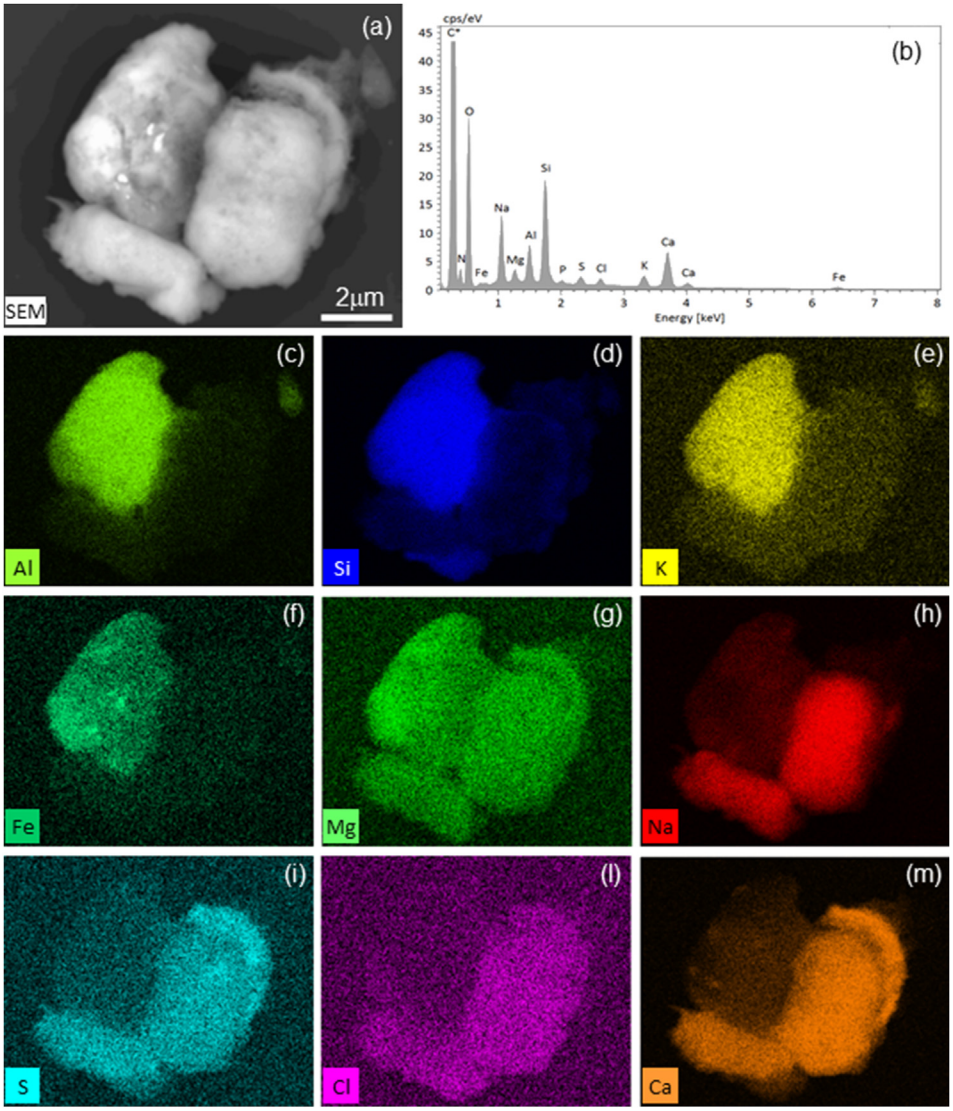

Figure 8. Elemental mapping of compound PM_{10} particles (sample 14/10): (a) SEM-BSE image showing at least three different particles and some brighter inclusions within the particle in the upper left; (b) averaged EDX spectrum; (c)–(m) single element maps. Note that Al, Si, K, and Fe (c–f, respectively) are concentrated in the upper left of the particle, whereas Na, S, Cl, and Ca (h–m, respectively), are concentrated in the particles in the lower right; Mg (g) is present along with P (map not shown). Fe (f) is concentrated in the inclusion within the upper left particle (arrows). Finally, Na (h) is not present in the curved particle in the upper right, whereas Mg (g), S (i), Cl (l), and Ca (m) are abundant.

small number of particles containing barium sulphate was present on the bees collected across all months.

4. Discussion

All the investigated honey bee samples from the monitoring station were remarkably "dirty", i.e., the bees had accumulated large amounts of airborne PM, while the control bees did not display any PM contamination. For the contaminated bees, the density of particles ranged from a few thousand to several hundreds of thousands per mm^2; however, this difference was primarily attributable to differing image magnifications rather than actual differences in PM concentrations. In general, low-magnification images tended to underestimate fine and ultrafine particles, while high-magnification images obscured coarser particles. Ultrafine particles ($PM_{0.1}$) did not contribute much to the overall PM mass, although they contributed considerably to the total number of particles (Donaldson et al., 2001; Kurth et al., 2014).

Most of PM accumulated on bees could be interpreted as naturally derived minerals, such as quartz, phyllosilicates, calcite, and feldspars from the surrounding alluvial deposits and agricultural soils. Calcite and clay minerals were found in all samples and, along with quartz, are by far the most abundant mineral phases in the silty clays and sandy silts that comprise the alluvial deposits of the Taro River and the Parma Stream. These waterways originate in the numerous Flysch formations of the Apennines that feed the alluvial deposits of the Po Valley on the southern side of the Po River. Agricultural activities, especially those involving the harvesting and sowing of wheat and alfalfa near the hive, may have contributed to the spread of minerals from the soils. However, the abundance of clay minerals and calcite was highly variable over time. This suggests the influence of further human activities, such as municipal waste incineration. Calcite is indeed one of the most common phases found on incinerator bottom ash, but further work is needed to assess the specific contributions of waste-treatment process including the removal and disposal of ash. The incinerator plant could also be responsible for the presence of airborne quartz PM, as SiO_2 is often abundant in bottom ash (Alam et al., 2019; Tang et al., 2020). In the studied samples, quartz was typically more abundant than feldspar, although both are prevalent in sedimentary lithic rocks, particularly in silts and sands. A possible explanation is that feldspars are much more sensitive to weathering than quartz, and therefore, degrade to clay minerals more rapidly (Klein and Philpotts, 2016).

Other mineral phases frequently found were Fe compounds including Fe oxides, metallic Fe, and Fe -alloys. Fe oxides (and Fe hydroxides) can be very abundant in nature, especially in association with mafic and ultramafic rocks, lateritic horizons, and the alteration of sulphide ores; however, these compounds are not abundant in the outcrops in the study

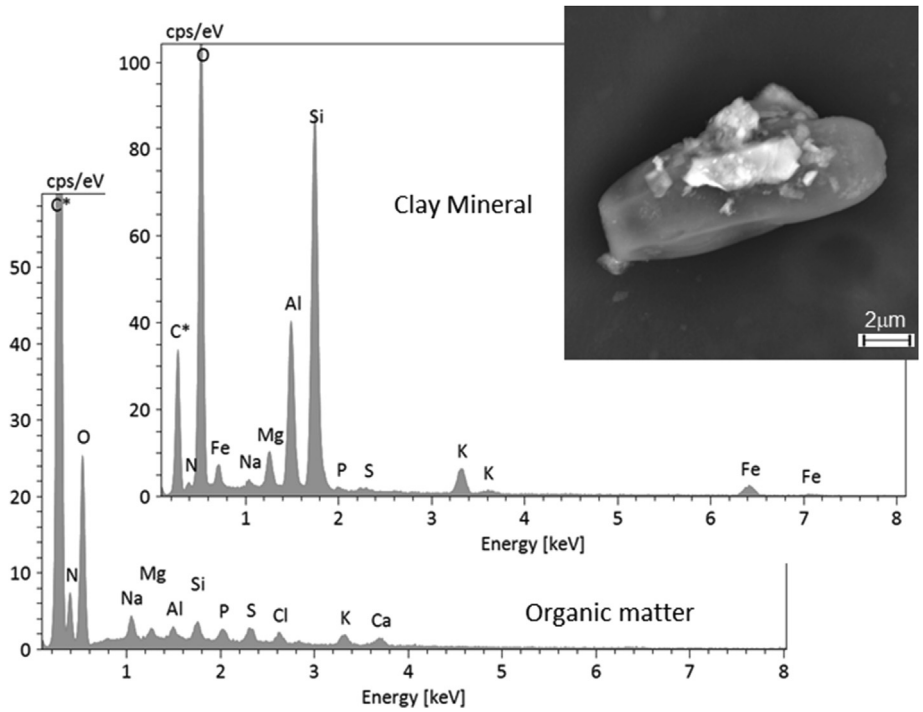

Figure 9. EDX spectra of a complex particle composed of clay minerals (upper spectrum, from the small bright particles in the inset) attached to an organic particle (lower spectrum, from the large dark particle in the inset).

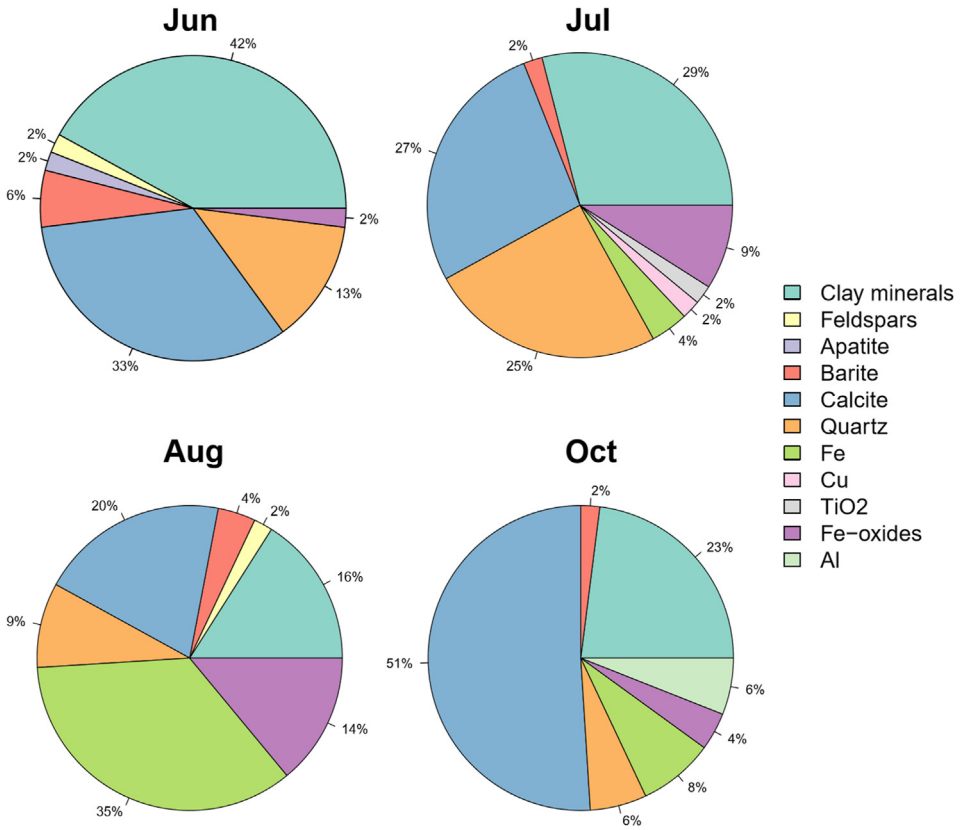

Figure 10. Pie charts representing the mineral abundances in the coarse PM fraction observed on honey bee wings. For consistency, only samples with a statistically significant number of analysed particles are reported: (a) sample 22/06 (52 spectra attributed); (b) sample 20/07 (48 spectra); (c) sample 10/08 (55 spectra); and (d) sample 14/10 (49 spectra).

area, which are largely Flysch rock. Metallic Fe is rare and may reach the Earth's surface via siderite meteorites in small quantities. Similarly, natural Fe alloys, in particular Fe–Ni alloys, may have an extra-terrestrial origin, and therefore, are very rare. In contrast, metallic Fe and Fe alloys derived from anthropogenic activities can be very abundant in the environment, being present in various manufactured goods (Gonet and Maher, 2019). For example, materials containing Fe are commonly used in the automotive industry (Carrero et al., 2014; Gonet and Maher, 2019). Thus, the Fe compounds identified in the study area may originate from the wearing of the mechanical parts of vehicles travelling on the adjacent A1 motorway. Other occasionally detected metallic particles, such as Cu and Al particles, may have similar origins, as they are otherwise considered rare (Cu) or absent (Al) in nature but are widely used in electric circuitry (Cu) and in the lighter chassis and engine parts of vehicles (Al). In July and August, tourism-related road traffic is particularly high due to the summer holiday season, often resulting in frequent traffic jams. In 2017, between the end of July and the first two weeks of August, during the "summer exodus", light vehicle traffic on the motorway increased by more than 50%, and the average daily number of light and heavy vehicles taking the nearby exit was 11,280 and 3,460, respectively (Autostrade per l'Italia S. p.A., traffic report). Thus, during this peak traffic period, bees collected on August 10 would have been exposed to increased levels of metal-bearing PM (relative to bees collected on July 20).

Another mineral phase frequently found on the bee wings was barite, a Ba sulphate. Barite is not rare in nature but is concentrated in hydrothermal deposits; therefore, it must be rare in the study area. Barite is, however, commonly used as a filler in various manufactured objects including vehicle tires and brakes. In particular, barite is the major chemical phase of break-pad material and is used as a filler to improve thermal and noise properties as well as wear resistance (Österle et al., 2001; Neis et al., 2017; Menapace et al., 2018). In this study, barite was present in all samples, and always as part of the <1 μm size fraction. This is in agreement with previous studies demonstrating that, when abraded from brakes and tyres, the grain size of barite is significantly reduced to the nanometre scale (Österle et al., 2001; Pellecchia and Negri, 2018; Papa et al., 2020).

Round, non-crystalline SiO_2 dust found on the bee wings could be linked to high-temperature combustion, such as that occurring at the nearby incinerator plant. According to the European Waste Incineration Directive, incinerator combustion must be conducted at above 850 °C to ensure the proper breakdown of toxic organic substances such as dioxins (Directive 2000/76/EC). Under such conditions, silicate matter may melt, and rapid post-combustion cooling can result in the formation of spherical PM (Kutchko and Kim, 2006; Alam et al., 2019).

An anthropogenic origin is also suggested for Ti oxide. Titanium dioxide, occurring as rutile, is not rare in nature and may concentrate in the heavy fraction of sediments. Yet, synthetic TiO_2 is widely used as a filler and whitening agent in various manufactured objects, such as plastics and paints, and is abundant in vehicle components.

Phosphorous was a minor but common element in the studied samples, generally associated with other elements as N, Cl, S. In one case, the observed spectrum was consistent with apatite [$Ca_5(PO_4)_3(OH,F,Cl)$]. Apatite, one of the main constituents of bones (Hughes and Rakovan, 2002), is an accessory mineral in many types of rocks, and can occur at relatively high concentrations in igneous and marine sedimentary rocks. Apatite is not, therefore, expected to be naturally abundant in the study area. Given the prevalence of phosphate-based fertilisers, the observed apatite may have had a secondary origin stemming from reactions between phosphates and Ca-compounds (Moore et al., 2004; Arai and Sparks, 2007; Shen et al., 2011). For example, such nutrients are needed in large quantities by *Medicago sativa*, a widespread crop in the study area, as low nutrient availability reduces the yield and persistence of this perennial plant (Berg et al., 2005).

We hypothesised that the background N, Si, P, S, Cl, K ±Al, ±Na, ±Mg, and ±Fe peaks obtained for the measured smaller particles (i.e., <1 μm in diameter) were signals from the honey bee wings components, including the cuticle and the haemolymph. The cuticle is primarily composed of chitin (a long-chain polymer with the composition $(C_8H_{13}O_5N)_n$) microfibers fixed in a protein matrix, e.g., hydrophobic proteins, with alanine ($C_3H_7NO_2$) as the predominant amino acid (Micas et al., 2016; Falcon et al., 2019) and resilin, an elastomeric protein with proline ($C_5H_9NO_2$) and glycerine ($C_2H_5NO_2$) as principal amino acids (Ma et al., 2015). Insect haemolymph comprises water, inorganic salts (mostly Na, Cl, K, Mg, and Ca), and organic compounds (carbohydrates, proteins, and lipids). Trehalose ($C_{12}H_{22}O_{11}$) and glucose ($C_6H_{12}O_6$) are the major circulating carbohydrates, and fatty acids, diglycerides, triglycerides, and phospholipids are major lipids in the haemolymph (Mikulecky and Bounias, 1997). While C, H, and O are major constituents of all these lipids, P is a minor constituent of phospholipids. Key proteins in adult bee haemolymph are transferrin, an Fe(III) transporter; apolipophorin, a lipid transporter; and vitellogenin, a nutrient-storage protein (Chan et al., 2006). P and S are minor constituents of these organic compounds. Therefore, C, H, O, and to a lesser extent, N, are major elements in honey bee wings, which is consistent with the EDX spectral features observed for small particles (PM_1). All other background elements, with the possible exception of Si and Al, are minor elements in the aforementioned wing components and consistently appeared in the spectra at very low concentrations.

In many cases, the spectra generated for very fine particles were dominated by Cl, S, or N peaks. At least in some cases, these elements could represent chlorides, SO_x, and NO_x as well as ammonia stemming from vehicle exhaust gas and incinerator emissions. These compounds may condense either directly onto honey bee wings or on fine airborne PM, such as clay minerals, that acts as condensation nuclei before accumulating on bees. This might explain the recurrent association of the background peaks with Na, Mg, Al, Si, and K. In other cases, background peaks were associated with Fe or Ba, suggesting that fine particles of iron or barite, respectively, may have acted as condensation nuclei. Detailed results and implications relating to fine and ultrafine particles are reported elsewhere (Papa et al., 2020).

P, K, and N are also major constituents of fertilisers (Gowariker et al., 2008), and Cl, P, S, and N (and Br and F) may be present in pesticides used in beekeeping and/or applied to crops (Ravoet et al., 2015). These substances may contaminate the bodies directly when bees visit inflorescences during foraging or, in a manner similar to vehicle exhaust gas and incinerator emissions, may be present in the atmosphere as aerosols and condense either directly onto bee wings or suspended fine mineral particles later collected by the bees. However, as our discussion demonstrates, the precise identification and provenance of fine particles continue to pose challenges.

5. Conclusions

Our results provide evidence of the presence of specific inhalable and respirable airborne PM (i.e., dust able to pass beyond the larynx and ciliated airways, respectively) in the study area. The honey bees analysed were highly contaminated with PM_{10} and $PM_{2.5}$ primarily comprising quartz, calcite, clay minerals, Fe-bearing PM, including iron oxides/hydroxides, metallic iron, Fe alloys, and barite.

Our data suggest that people living in the area are subjected to chronic (continuous/repeated) exposure to specific airborne PM emitted by vehicular traffic, local agricultural operations, and waste incineration, and exposure levels may vary rapidly based on recurrent local activities. For example, the increase in natural mineral compounds (e.g., clay minerals, calcite, and quartz) was closely linked to cultivation cycles, while metal-bearing PM abundance increased in conjunction with periods of elevated local road traffic.

In view of the recent COVID-19 outbreak occurring in Italy and centred in the Po Valley, it is also important to verify the possible association between the outbreak of respiratory viruses and exposure to specific components of airborne PM. More particle identification and

classification data are needed, therefore, alongside improved information on viral viability on specific airborne PM components.

Declarations

Author contribution statement

Ilaria Negri: Conceived and designed the experiments; Performed the experiments; Contributed reagents, materials, analysis tools or data; Wrote the paper.

Giancarlo Capitani: Performed the experiments; Analyzed and interpreted the data; Contributed reagents, materials, analysis tools or data; Wrote the paper.

Giulia Papa: Performed the experiments; Analyzed and interpreted the data.

Marco Pellecchia: Conceived and designed the experiments; Performed the experiments; Analyzed and interpreted the data; Contributed reagents, materials, analysis tools or data; Wrote the paper.

Funding statement

This work was supported by the ECORESILIENTE project of the Università Cattolica del Sacro Cuore (Italy) (I.N.). G.P. was partially supported by the Doctoral School on the Agro-Food System (Agrisystem) of the Università Cattolica del Sacro Cuore (Italy).

Data availability statement

Data will be made available on request.

Declaration of interests statement

The authors declare no conflict of interest.

Additional information

Supplementary content related to this article has been published online at https://doi.org/10.1016/j.heliyon.2021.e06194.

Acknowledgements

We thank Dr. Alice Dondè and Dr. Antonia Desiante for their support during the data collection.

References

Alam, Q., Schollbach, K., van Hoek, C., van der Laan, S., de Wolf, T., Brouwers, H.J.H., 2019. In-depth mineralogical quantification of MSWI bottom ash phases and their association with potentially toxic elements. Waste Manag. 87, 1–12.

Arai, Y., Sparks, D.L., 2007. Phosphate Reaction Dynamics in Soils and Soil Components: A Multiscale Approach.

Bargańska, Ż., Ślebioda, M., Namieśnik, J., 2016. Honey bees and their products: bioindicators of environmental contamination. Crit. Rev. Environ. Sci. Technol. 46, 235–248.

Bencsik, A., Lestaevel, P., Guseva Canu, I., 2018. Nano- and neurotoxicology: an emerging discipline. Progr. Neurobiol. 160, 45–63.

Berg, W.K., Cunningham, S.M., Brouder, S.M., Joern, B.C., Johnson, K.D., Santini, J., Volenec, J.J., 2005. Influence of phosphorus and potassium on alfalfa yield and yield components. Crop Sci. 45 (1).

Bonmatin, J.-M., Giorio, C., Girolami, V., Goulson, D., Kreutzweiser, D.P., Krupke, C., et al., 2015. Environmental fate and exposure; neonicotinoids and fipronil. Environ. Sci. Pollut. Control Ser. 22 (1), 35–67.

Brown, J.S., Gordon, T., Price, O., Asgharian, B., 2013. Thoracic and respirable particle definitions for human health risk assessment. Part. Fibre Toxicol. 10 (1), 12.

Calabrese, L., Ceriani, A., 2009. Note illustrative della carta geologica d'Italia alla scala 1 : 50.000 : Foglio 181 : Parma Nord (ISPRA - Istituto Superiore per la Protezione e la Ricerca Ambientale Regione Emilia-Romagna Servizio geologico d'Italia, ed.). Firenze.

Carrero, J.A., Arana, G., Madariaga, J.M., 2014. Chapter 6. Use of Raman spectroscopy and scanning electron microscopy for the detection and analysis of road transport pollution. In: Spectroscopic Properties of Inorganic and Organometallic Compounds, 45, pp. 178–210.

Chan, Q.W.T., Howes, C.G., Foster, L.J., 2006. Quantitative comparison of caste differences in honeybee hemolymph. Mol. Cell. Proteomics 5 (12), 2252–2262.

Devillers, J., Pham-Delegue, M.-H., 2002. Honey Bees: Estimating the Environmental Impact of Chemicals. Taylor and Francis, London.

Donaldson, K., Stone, V., Clouter, A., Renwick, L., MacNee, W., 2001. Ultrafine particles. Occup. Environ. Med. 58 (3), 211–216.

Falcon, T., Pinheiro, D.G., Ferreira-Caliman, M.J., Turatti, I.C.C., Abreu, F.C.P. de, Galaschi-Teixeira, J.S., Martins, J.R., Elias-Neto, M., Soares, M.P.M., Laure, M.B., Figueiredo, V.L.C., Lopes, N.P., Simões, Z.L.P., Garófalo, C.A., Bitondi, M.M.G., 2019. Exploring integument transcriptomes, cuticle ultrastructure, and cuticular hydrocarbons profiles in eusocial and solitary bee species displaying heterochronic adult cuticle maturation. PloS One 14, e0213796.

Giglio, A., Ammendola, A., Battistella, S., Naccarato, A., Pallavicini, A., Simeon, E., Tagarelli, A., Giulianini, P.G., 2017. *Apis mellifera ligustica*, Spinola 1806 as bioindicator for detecting environmental contamination: a preliminary study of heavy metal pollution in Trieste, Italy. Environ. Sci. Pollut. Control Ser. 24, 659–665.

Garrido, P.M., Martin, M.L., Negri, P., Eguaras, M.J., 2013. A standardized method to extract and store haemolymph from Apis mellifera and the ectoparasite Varroa destructor for protein analysis. J. Apicult. Res. 52 (2), 67–68.

Gonet, T., Maher, B.A., 2019. Airborne, vehicle-derived Fe-bearing nanoparticles in the urban environment: a review [Review-article]. Environ. Sci. Technol. 53 (17), 9970–9991.

Goretti, E., Pallottini, M., Rossi, R., La Porta, G., Gardi, T., Cenci Goga, B.T., et al., 2020. Heavy metal bioaccumulation in honey bee matrix, an indicator to assess the contamination level in terrestrial environments. Environ. Pollut. 256, 113388.

Gowariker, V., Krishnamurthy, V.N., Gowariker, S., Dhanorkar, M., Paranjape, K., 2008. The Fertilizer Encyclopedia. John Wiley and Sons, Inc, Hoboken, NJ, USA.

Hughes, J.M., Rakovan, J., 2002. The crystal structure of apatite, Ca5(PO4)3(F,OH,Cl). Rev. Mineral. Geochem. 48 (1), 1–12.

Klein, C., Philpotts, A., 2016. Earth Materials: Introduction to Mineralogy and Petrology, second ed.

Kurth, L.M., McCawley, M., Hendryx, M., Lusk, S., 2014. Atmospheric particulate matter size distribution and concentration in West Virginia coal mining and non-mining areas. Mod. Pathol. 27 (8), 405–411.

Kutchko, B.G., Kim, A.G., 2006. Fly ash characterization by SEM – EDS, 85, 2537–2544.

Ma, Y., Ning, J.G., Ren, H.L., Zhang, P.F., Zhao, H.Y., 2015. The function of resilin in honeybee wings. J. Exp. Biol. 218, 2136–2142.

Micas, A.F.D., Ferreira, G.A., Laure, H.J., Rosa, J.C., Bitondi, M.M.G., 2016. Proteins of the integumentary system of the honeybee, *Apis mellifera*. *Arch. Insect Biochem.* Physiol. 93, 3–24.

Maher, B.A., Ahmed, I.A.M., Karloukovski, V., MacLaren, D.A., Foulds, P.G., Allsop, D., Calderon-Garciduenas, L., 2016. Magnetite pollution nanoparticles in the human brain. Proc. Natl. Acad. Sci. Unit. States Am. 113 (39), 10797–10801.

Marcazzan, G.M., Vaccaro, S., Valli, G., Vecchi, R., 2001. Characterisation of PM10 and PM2.5 particulate matter in the ambient air of Milan (Italy). Atmos. Environ. 35 (27), 4639–4650.

Menapace, C., Leonardi, M., Matėjka, V., Gialanella, S., Straffelini, G., 2018. Dry sliding behavior and friction layer formation in copper-free barite containing friction materials. Wear 398–399, 191–200.

Mikulecky, M., Bounias, M., 1997. Worker honeybee hemolymph lipid composition and synodic lunar cycle periodicities. Braz. J. Med. Biol. Res. 30 (2), 275–279.

Moore, R.C., Sanchez, C., Holt, K., Zhang, P., Xu, H., Choppin, G.R., 2004. Formation of hydroxyapatite in soils using calcium citrate and sodium phosphate for control of strontium migration. Radiochim. Acta 92 (9–11).

Negri, I., Mavris, C., Di Prisco, G., Caprio, E., Pellecchia, M., 2015. Honey bees (*Apis mellifera*, L.) as active samplers of airborne particulate matter. PloS One 10 (7), 1–22.

Neis, P.D., Ferreira, N.F., Fekete, G., Matozo, L.T., Masotti, D., 2017. Towards a better understanding of the structures existing on the surface of brake pads. Tribol. Int. 105, 135–147.

Osterle, W., Griepentrog, M., Gross, T., Urban, I., 2001. Chemical and microstructural changes induced by friction and wear of brakes. Wear 251 (1–12), 1469–1476.

Papa, G., Capitani, G., Capri, E., Pellecchia, M., Negri, I., 2020. Vehicle-derived ultrafine particulate contaminating bees and bee products. Sci. Total Environ. 141700.

Pellecchia, M., Negri, I., 2018. Particulate matter collection by honey bees (*Apis mellifera*, L.) near to a cement factory in Italy. PeerJ 2018 (7), 1–21.

Perugini, M., Manera, M., Grotta, L., Abete, M.C., Tarasco, R., Amorena, M., 2011. Heavy metal (Hg, Cr, Cd, and Pb) contamination in urban areas and wildlife reserves: honeybees as bioindicators. Biol. Trace Elem. Res. 140, 170–176.

Pirovano, G., Colombi, C., Balzarini, A., Riva, G.M., Gianelle, V., Lonati, G., 2015. PM2.5 source apportionment in Lombardy (Italy): comparison of receptor and chemistry-transport modelling results. Atmos. Environ. 106, 56–70.

Ravoet, J., Reybroeck, W., de Graaf, D.C., 2015. Pesticides for apicultural and/or agricultural application found in Belgian honey bee wax combs. Bull. Environ. Contam. Toxicol. 94 (5), 543–548.

Rühlmann, J., Körschens, M., Graefe, J., 2006. A new approach to calculate the particle density of soils considering properties of the soil organic matter and the mineral matrix. Geoderma 130 (3–4), 272–283.

Setti, L., Passarini, F., De Gennaro, G., Barbieri, P., Perrone, M.G., Borelli, M., et al., 2020. SARS-Cov-2RNA found on particulate matter of Bergamo in Northern Italy: first evidence. Environ. Res. 188, 109754.

Shen, J., Yuan, L., Zhang, J., Li, H., Bai, Z., Chen, X., et al., 2011. Phosphorus dynamics: from soil to plant. Plant Physiol. 156 (3), 997–1005.

Tang, Z., Li, W., Tam, V.W.Y., Xue, C., 2020. Advanced progress in recycling municipal and construction solid wastes for manufacturing sustainable construction materials. *Resour. Conserv. Recycl.* X 6, 100036.

Vaknin, Y., Gan-Mor, S., Bechar, A., Ronen, B., Eisikowitch, D., 2000. The role of electrostatic forces pollination. Plant Systemat. Evol. 222 (1–4), 133–142.
van Doremalen, N., Bushmaker, T., Morris, D.H., Holbrook, M.G., Gamble, A., Williamson, B.N., Munster, V.J., 2020. Aerosol and Surface Stability of SARS-CoV-2 as Compared with SARS-CoV-1. New England Journal of Medicine. NEJMc2004973.
Wang, Y., Eliot, M.N., Wellenius, G.A., 2014. Short-term changes in ambient particulate matter and risk of stroke: a systematic review and meta-analysis. J. Am. Heart Assoc. 3 (4), 1–22.